Utilization of Unmanned Aerial Vehicle (UAV) for Tidal Flood Study Related to Land Subsidence in Muara Angke, North Jakarta

Riza Aitiando Pasaribu[1], Dea Fauzia Lestari[1], Nadya Cakasana[1], Muhammad Abdul Ghofur Al Hakim[2], Farel Ahadyatulakbar Aditama[2], Joachim Yehezkiel Corry Lawoliyo[3], Fida Zalfa Lathifah Yasmin[3], Rizkyah Zahra Rani[3], Krisanda Sekar Kinanti[3], Muhammad Ravelino[3], Kayla Felisha Puspitasari[3]

[1]Lecturer, Department Marine Science and Technology, Faculty of Fisheries and Marine Sciences, IPB University

[2]Laboratorium Technician, Department Marine Science and Technology, Faculty of Fisheries and Marine Sciences, IPB University

[3] Student of International Program of Marine Science and Technology Study Program, Department Marine Science and Technology, Faculty of Fisheries and Marine Sciences, IPB University

Abstract

The Jakarta coastal location is placed in North Jakarta and borders the Java Sea. However, coral reefs have suffered widespread degradation in current years because of the effect of human disturbances and herbal elements on biodiversity and surroundings functions. It is thought that human sports cause 90% of coral reef harm and 10% is due to weather change. This could have an effect on excessive tidal waves, which purpose tidal flooding in coastal regions like Muara Angke. Land subsidence contributes to the phenomenon of tidal flooding in Jakarta. This tidal flood inundates components of the coastal plains or locations decrease than the excessive tide sea level. The method for determining the pool of water that floods the Muara Angke area is by knowing the highest tide and the slope of the area. This can make it easier to predict inundated areas. The tool used to detect the slope of the area using UAV. The results of a drone-based Digital Elevation Model (DEM) are more accurate. A tidal flood in Muara Angke is predicted to result in 5,82 ha using an elevation model. Increased exposure to flooding is a result of land subsidence. This is due to the HHWL's elevation of 0.73 meters above MSL. However, the Muara Angke loss estimate came to 99,5 million Rupiah, covering a total area of 2.72 ha and 0.43 ha (road).

Keyword: DEM, Flood, Land Subsidence, Tidal, UAV

Introduction

Jakarta is the capital city of Indonesia, which was formerly known as Nusantara. According to BPS (Badan Pusat Statistika), Jakarta will have 664,01 km^2 by 2021, and is located at latitude 6° 12' 0.0000" S and longitude 106° 48' 59.9976". Jakarta is divided into six regencies and cities, which are known as Kepulauan Seribu Island, North Jakarta, South Jakarta, West Jakarta, East Jakarta, and Jakarta City Center, with a total land area of 52,38 km^2. Following the Kepulauan Seribu dalam Angka 2021 (BPS, 2023), Jakarta has a population of 10.644.776 people. This devastated number places Jakarta at the highest population density in Indonesia, at 15,97 km2, while West Java province has a population density of 1,37 km^2 (Databoks).

The Jakarta coastal area is located in North Jakarta and borders the Java Sea. However, coral reefs have suffered significant degradation in recent years as a result of the impact of human disturbances and natural factors on biodiversity and ecosystem functions. It is known that human activities cause 90% of coral reef damage and 10% is caused by climate

change (natural events) (Harahap *et al.* 2021), and mangrove deforestation and degradation are occurring at alarming rates (Arifanti 2020). Climate change is defined as a significant change in average weather conditions, such as becoming warmer, wetter, or drier over several decades or longer. The longer-term trend distinguishes climate change from natural weather variability.

Global sea level rose by 16 cm between 1902 and 2015. Due to increasing

to prevent coastal phenomena that cause problems for society.

Unmanned Drone One type of hardware technology is an aerial vehicle, also known as a flying robot (Azmi et al 2020). The drone was first used for military purposes in 1849 according to records. The first UAVs were developed during World War I as aerial torpedoes, which are now known as cruise missiles (Kim *et al.* 2017). Drones are now widely used for a variety of other purposes, including search and
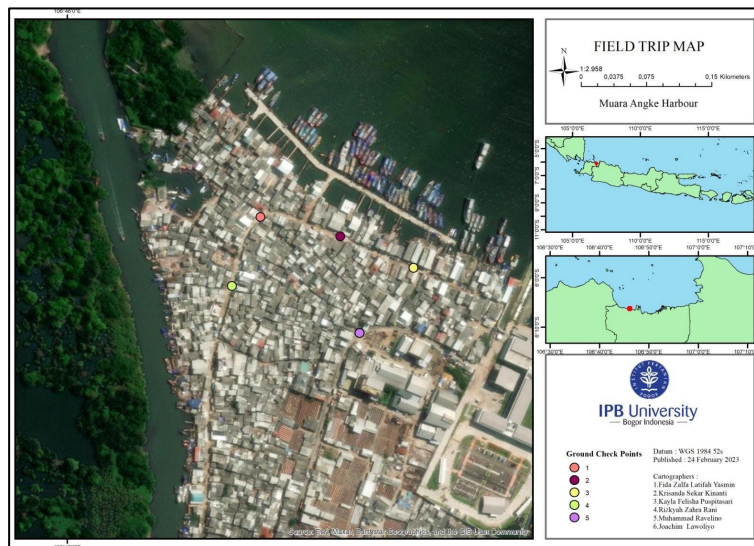

Figure 1. Research Location and Ground Check Points Map

rates of ice loss from the Greenland and Antarctic ice sheets, sea-level rise has accelerated in recent decades. The amount of sea-level rise to 2050 (0.24-0.32 m) (Priestley *et al*. 2021) and potentially cover up to 1045 Ha land (Damayati 2016) is one of the most significant caused by climate change (Mimura 2013). This can have an impact on high tidal waves, which cause tidal flooding in coastal areas like Muara Angke. Tidal flooding occurs when seawater enters the mainland as a result of high tides (Hadi 2017).

Land subsidence contributes to the phenomenon of tidal flooding in Jakarta. This tidal flood inundates parts of the coastal plains or places lower than the high tide sea level (Karana and Supriharjo 2013). However, understanding sea-level rise is one of the red flags to look out for in order

rescue, surveillance, traffic monitoring and weather, fire suppression, agriculture, personal use, and shooting (O'Donnel 2017). Despite this, drones are expected to have a significant impact on remote sensing sections, whether for agriculture or public recreation.

According to Oktafiana 2021, drones produce higher-resolution imagery and are easy to transport outside. Regardless of the cost, the drone is used to provide good-fine resolution and data-capture certain elements such as land inclination, which is manually measured by a clinometer (Oktafiana 2021). In addition to the benefits mentioned above, drones have been used to assist researchers in sorting out hydrology issues or land conservation at geomorphological issues. Thus, in this study, the UAV is intended to produce a

Digital Elevation Model (DEM), which will be fed into the terrain filter method to produce a Digital Terrain Model (DTM) and a Digital Surface Model (DSM).

Method

Materials and Tool

The tool used is a DJI Panthom 4 drone, a smartphone with DJI GO and Drone Deploy apps, a stationary, Ground CheckPoint banner, and equipped laptops with Microsoft Office software, ArcGIS 10.3, Agisoft PhotoScan Professional 64bit, and Terrain Filter PCI Geomatica 2014, as well as a smartphone with Avenza Map and Mobile Topographer applications.

Time and Location

This study will take place on Jl. Muara Angke, Pluit, Kec. Penjaringan, Jkt Utara, Daerah Khusus Ibukota Jakarta on March 18, 2023. The Ground Check Points that will be used are as follows (Figure 1):

The DJI Phantom 4 drone will be used for aerial photography, with a total of six Ground Check Points. The following is the flight plan for the Drone Deploy at the 6 Ground Check Points (Figure 2). There will be 291 images that will be taken later. Furthermore, the image data fromthe drone will be processed using the Agisoft PhotoScan Professional 64bit and Terrain Filter PCI Geomatica 2014 software to produce a DEM.
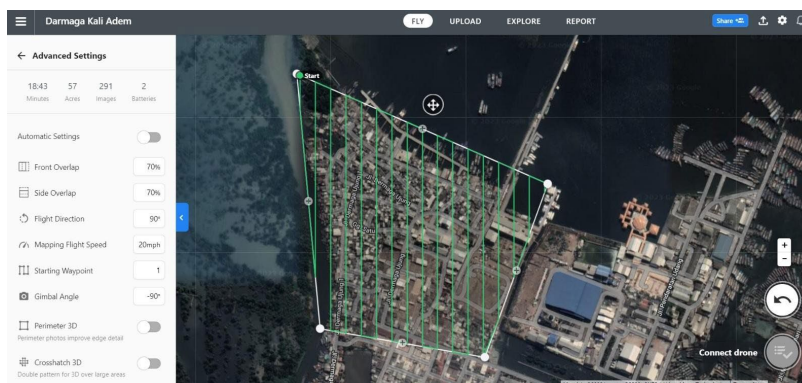

Figure 2. Map of Drone Deploy Plan

Analysis Data

DEM is divided into two parts: the Digital Surface Model (DSM) and the Digital Terrain Model (DTM). However, according to Oktafiana 2021, the aerial photo extraction process includes several stages, including: aligning or merging aerial photos, orthorectification, process build dense, build mesh, build DEM, and then exporting the output into orthophoto mosaic and DSM. At this point, aerial photographs are processed with the Agisoft software PhotoScan Professional 64 bit. First, the align photos process is carried out, which aims to display aerial photography of its flight path and arrange the patch. At this stage, aerial photographs are identified based on camera position and orientation according to coordinates, resulting in a tie point model.

Drone Analysis Data

The next step is to create a dense cloud build, which will serve as the foundation for the mesh construction process. The mesh data is then converted into DSM (Digital Surface Model) raster data using the DEM build tool. The DSM generated in this process represents the elevation value surface (surface), which includes terrain elevation (on land without vegetation and buildings) and canopy elevation (on vegetated land and awakened). The build mesh stage results are also used in the orthomosaic build process,

which produces orthophoto mosaic. The processing outcomes are The DSM and orthophotos are then exported to geoTIFF format.

Terrain Filter creates the Digital Terrain Model alongside the coin. This software allows you to create DTMs either automatically or manually, and it is useful for research. This method is chosen by hand, specifically by using the terrain filter flat method. The manual method in this software has two options: the flat terrain filter, which is used in areas dominated by rice fields, such as in area research or urban areas, and the terrain rough filter, which is used in hilly terrain. The first step is to manually digitize the area where the terrain value is desired. This digitization (ground area) must be done carefully, or it will result in a poor DTM value. In addition, the flat terrain filter method is used to generate data DTM across the research area. As a result, the flowchart provided below interprets the entire process of this research (Figure 3).
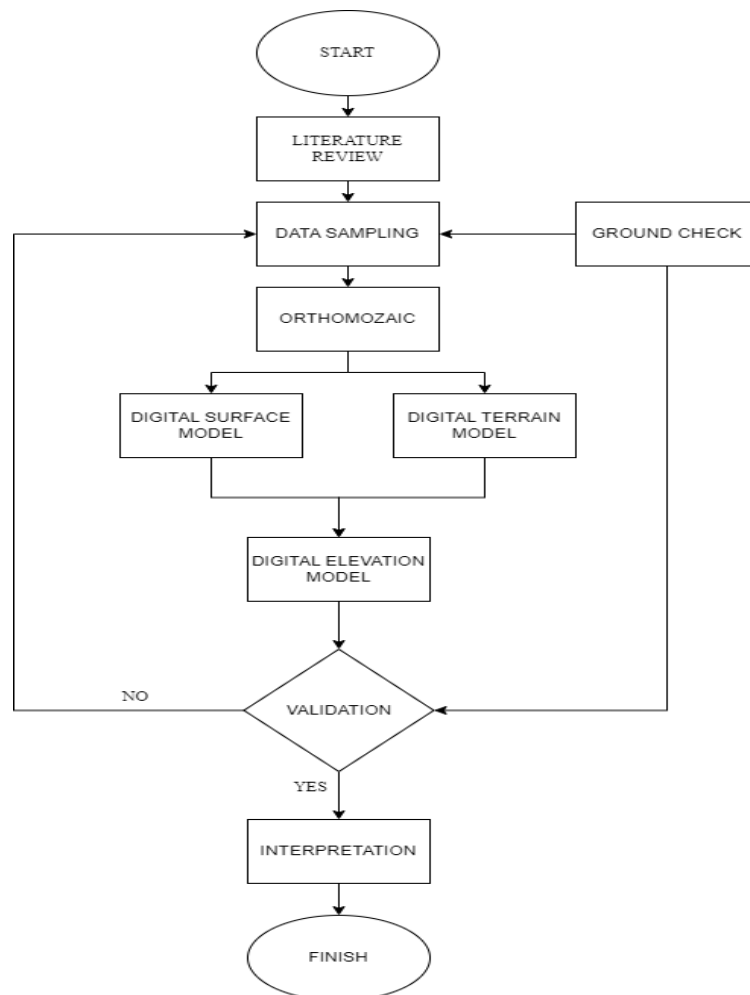

Figure 3. Research Flowchart

Sea Level Data Analysis

The least square method is used to calculate high and low sea level data. The formula (1) for the least square method is as follows:

$$v = \sum_{i'=0}^{3} \left[\begin{array}{l} Gi'^{(\theta)} \sum_{j'k'l'm'n'} A'(j'k'l'm'n') \cos(2\pi V_a) \\ +Gi'(\theta) \sum_{j'k'l'm'n'} B'(j'k'l'm'n') \cos(2\pi V_a) \end{array} \right] \dots\dots\dots\dots\dots(1)$$

G and G' are geodetic functions with type i' (slow, diurnal, andsemi-diurnal types are 0,1,2) and latitude θ, A', and B' as Doodson numbers; Va as an astronomical argument, and j'k'l'm'n' as a Doodson number with a certain constant. The following (Table 1) formula reference is used to determine the type of high tide component that occurs:

Table 1. Tidal Components Formula

No	Description		Formula
i.	Mean High Water Spring	:	Sun + (AM2 + AS2)
ii.	Mean Low Water Spring	:	Sun – (AM2 + AS2)
iii.	Highest High Water Spring	:	Sun + (AM2 + AS2+AK1 + AO1)
iv.	Lowest Low Water Spring	:	Zo - (AM2+AS2+AK1 + AO1)
v.	Highest Astronomical Tide	:	Zo + Σai
vi.	Lowest Astronomical Tide	:	Zo –Σai

Result

Orthomozaic Map

WebODM software was used to create an entire orthophoto map. The initial phase was the labeling process, which included all of the chosen building locations modified with the personalized description. The labeling result for each building included the Industrial area, which is shown in the Industrial Map (Figure 4).

The next step was to use a map layout editor to generate the best resolution for the orthophoto map. The orthophoto map resulted in a size of 2,2 M - 3,7 M. This is due to the fact that the photo was taken at an elevation of 80 meters above ground.

Spot-taking UAV imagery is influenced by atmospheric windows such as sunlight, and this can also be false-valued due to the boundary and stitching process in the orthomosaic process (Kaamin *et al.* 2022). In comparison to the UAV result, Sentinel-2 carries the Multispectral Imager (MSI). This sensor provides 13 spectral bands with pixel sizes ranging from 10 to 60 meters. The orientation of the map was changed to landscape, and boundaries were added to ensure that it fit within the margins (Ameer and Gazal 2021).
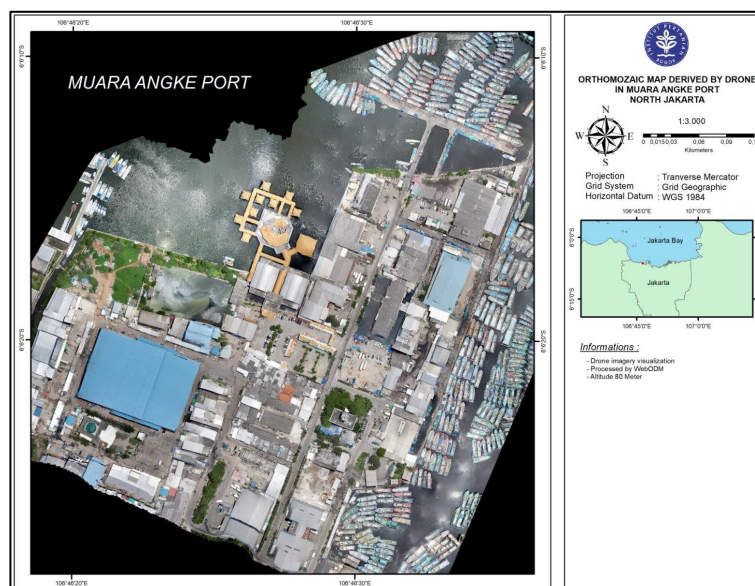

Figure 4. Orthomosaic map derived by drone in Muara Angke Port, North Jakarta

Digital Elevation Model

The orthomosaic was processed to obtain the Digital Elevation Model (DEM) (Figure 5), which was then automatically led to the Digital Terrain Model (DTM) and Digital Surface Model (DSM). However, the DEM is divided into seven classes, with the area below zero meters line-contoured to contrast the result, and the reddish area performing best. Elevation was corrected by comparing the Ground Check Point (GCP), resulting in a more detailed and precise area. Tachymetry-generated DEMs have the highest accuracy, followed by RTK-GPS and TLS (Arif et al 2018). Despite the fact that the DEM is considered high-accuracy, the water in Figure 5 was stretched higher than the lands. However, the water body was reclassified in ArcMap using the Analysis tool. Aeolian force and sea surface roughness caused Digital Elevation Model (DEM) error (Duo et al 2021). However, DEM results are influenced by a variety of factors, including technical and environmental factors.
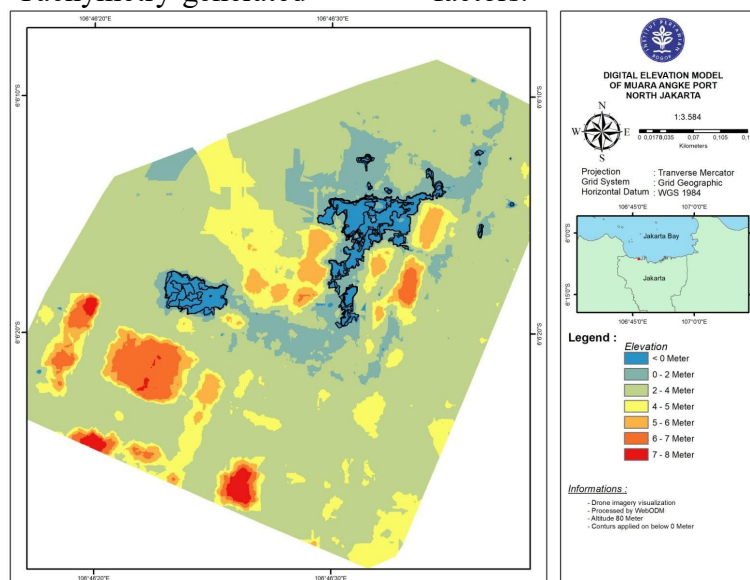

Figure 5. Digital elevation model of Muara Angke Port North Jakarta

Tidal Flood in Muara Angke Port North Jakarta

Tides are the periodic motion of seawater caused by the combined gravitationaleffects of the moon and the sun as they change position relative to the rotating earth. Tide is the superposition of hundreds of tidal constituents, each having a frequency that is the sum and difference of five fundamental frequencies (Kusuma *et al.* 2021). The tide type in Muara Angke is mixed tide prevailing semidiurnal. In one day there are two high tides and two low tides, but the height and period are different. Mixed tide, prevailing semi-diurnal, for example, occurs in most of eastern Indonesian waters.

According to the graph below, the measurement resulted in 7.77 m of highest elevation and 6.467 m of lowest elevation, giving the MSL value of 0.73 M. Admiralty 29 was used for measurement, which brought certain harmonic components. This is due to the fact that the method developed by Rich Pawlowicz in 2002 yields a result spanning 9 values of the main tidal components (diurnal and semidiurnal). While the least squares method produces the most components, namely 68 tidal components that include diurnal, semidiurnal, and shallow water components (Ichasari *et al.* 2020). Highest Astronomical Tide (HAT) increased 2,3 m above MSL.
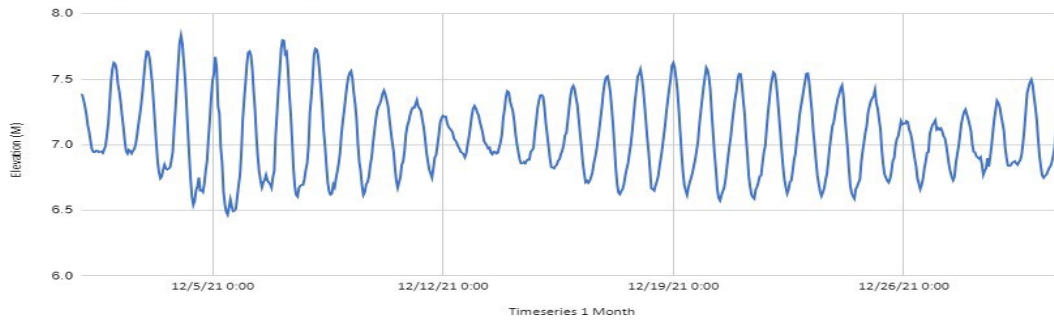
Figure 6. Tidal Graph in Muara Angke

The tidal flood area is divided into two classes, as shown in the figure below: 0.75 M and 2.25 M. This is due to the tidal calculation being divided into two classes: the Highest High Water Level (HHWL) is calculated for 0.75 M and the Highest Astronomical Tide (HAT) is calculated for 2.25 M. Data from 2000 to 2015 revealed that the average tidal height was 2.05 m, with the highest potential in 2030 being approximately 2.75 m (Hilmi et al 2021). However, based on previous research, the number of tidal performances supports the tidal flood phenomenon. As a result, the total area is 5,82 Ha2, which has a negative impact on settlement, market, industry, and houses.

Table 2. Result Tidal in Muara Angke

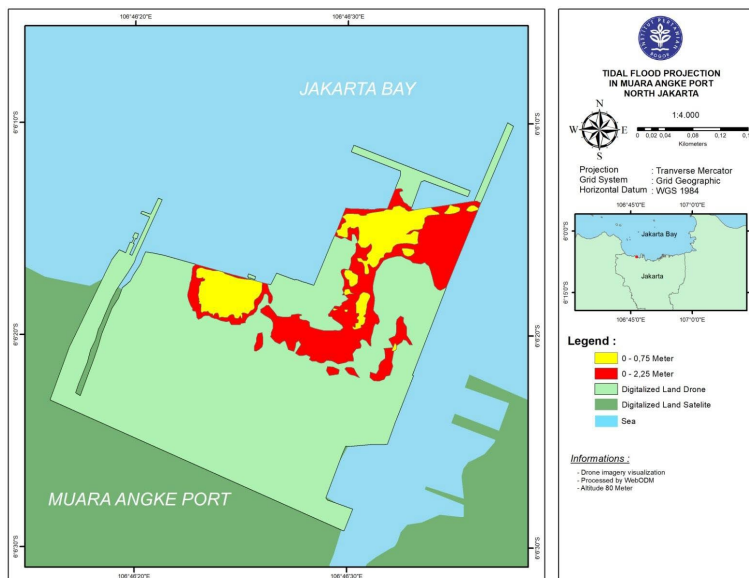| Description	MSL	LLWL	HHWL	Tidal range	HAT
Elevation (m)	7,06	6,47	7,77	1,36	9,38

Figure 7. Tidal Flood Projection of Muara Angke Port North Jakarta

Tidal Flood and Land Subsidence

Pointing to the Figure 7 below, 10 out of 22 tagged industrial buildings are projected to be covered by HAT tidal flood. Around 2,91 Ha is projected covered by 0,75 m (HHWL), whereas

several matrix and value estimation. According to the figure. 5, One of the main aspect land use coverage by flood is land subsidence. According to the projected sea level in the future coming,
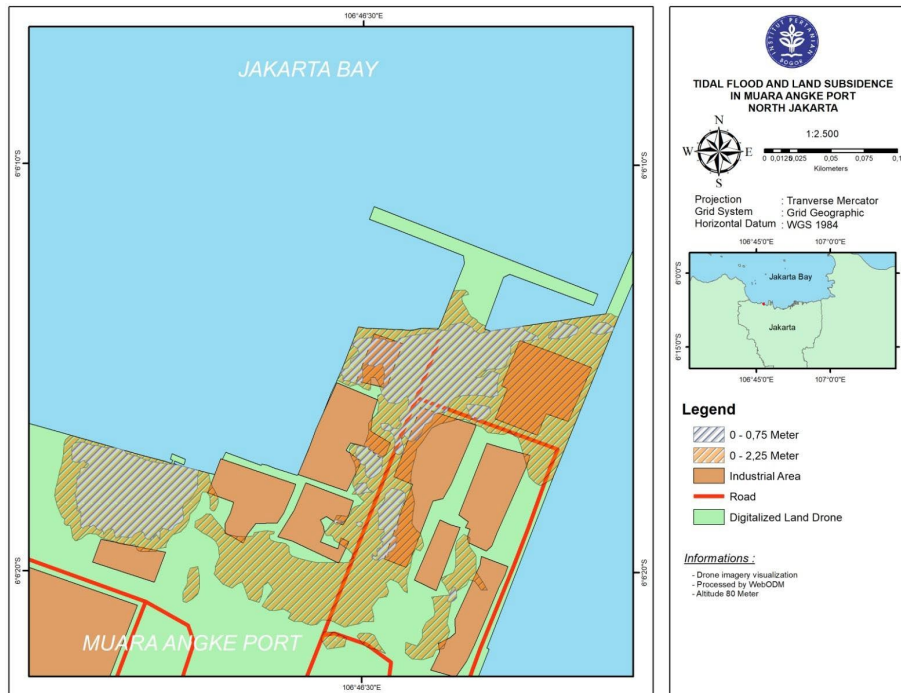

Figure 8. Tidal Flood Projection of Muara Angke Port North Jakarta

5,82 Ha covered with 2,25 m (HAT). According to a study conducted by Purnama et.al., 2015, North Jakarta has been classified as one of the highest industrial loss, which is proved by

Conclusion

Digital Elevation Model (DEM) by drone has more precise result comparing to satellite. Elevation model pointing tidal flood in Muara Angke results in 5,82 Ha. Land subsidence has a role in

there are 3 (three) significant mean sea level rise, with a higher total rise than the coastal elevation of Jakarta city in that period.

increasing flood exposure. This is because the HHWL is 0,73 Meter above the MSL. However, the loss estimation in Muara Angke resulted 99,5 Million Rupiah with total area covered 0.43 Ha (road) and 2.72 Ha (industrial areas).

REFERENCES

[BPS] Badan Pusat Statistika Indonesia. Jakarta. Accessed on 13 February 2023. Available on https://Jakarta.bps.go.id.

[Databoks] Portal of Economic and Business data statistic. Jakarta. Accessed on 13 February 2023. Available on https://databoks.katadata.co.id/.

Anggraeni Damayanti. 2016. Climate Change Impact Analysis Based on Sea Level Rise to Subaya city. Master Program

Departement of Environmental Engineering Faculty of Civil Engineering and Planning Sepuluh Nopember Insitute of Technology Surabaya. Accessed on 13 February 2023. Available on. https://repository.its.ac.id/71257/1/3314 201025-master-theses.pdf.

Arifanti VB. 2020. Mangrove management and climate change: a review in Indonesia. In IOP conference series: earth and environmental science. 487(1):012022.

Asniza Md Yunus, Abd Halim Hamzah, Fatin Afiqah Md. Azmi. 2020. Drone Techonology as A Modern Tool in Monitoring the Rural-Urban Development. IOP. Series: Earth and Environmental Science. 540(2020). doi:10.1088/1755-1315/540/1/012076.

Bang S., Kim H., & Kim H. 2017. UAV-based automatic generation of highresolution panorama at a construction site with a focus on preprocessing for image stitching - Automation in Construction (Seoul: Elsevier Ltd.) vol 84 p 70-80.

Harahap Syawaludin A. Nikita A. Shabrina Noir P Purba. Mega L. Syamsuddin. The patterns of changes in coral reef coverage (1994-2006) in the Seribu Islands National Park, Jakarta, Indonesia. World News of Natural Sciences 38 (2021): 120-138.

Intan Rohmatul Oktafiana. 2021. Analisi Data Drone untuk Membangun Digital Terrain Model (DTM). Deparment of land resource and science faculty of agriculture of Bogor Agricultural University.

Mimura N. 2013. Sea-level rise caused by climate change and its implications for society. Proceedings of the Japan Academy. 89(7): 281–301. doi: 10.2183/pjab.89.281

O'Donnell S. 2017. A Short History of Unmanned Aerial Vehicles. Available on https://consortiq.com/mediacentre/ blog/short-history-unmanned-aerialvehicles-uavs.

Priestley RK, Heine Z, Milfont TL. 2021. Public understanding of climate change-related sea-level rise. PLoS ONE. 16(7): e0254348. doi:10.1371/journal.pone.0254348

Speelman, E.N. 2009. The eocenicrctic arctic azolla bloom: environmental conditions, productivity, and carbon drawn down. Geobiology. 7, 155 – 170.